

an acceptor number for the solvent from the following equation

$$AN = 100(\delta_{\text{corr}})/\delta_{\text{corr}}(\text{SbCl}_5\text{-Et}_3\text{PO}) \quad (12)$$

where δ_{corr} is the ^{31}P NMR chemical shift of Et_3PO at infinite dilution in a solvent S. This chemical shift value is referenced to an infinitely dilute solution of Et_3PO in *n*-hexane and corrected for difference in volume susceptibilities between solvent S and *n*-hexane. Thus, for *n*-hexane $\delta_{\text{corr}} = 0$, but the measured value with respect to the external standard (after extrapolation to infinite dilution and correction for volume susceptibility differences) is -1.68 ppm, as shown in column 1 of Table III. The denominator of eq 12 denotes the corresponding chemical shift value for the adduct $\text{SbCl}_5\text{-Et}_3\text{PO}$ at infinite dilution in 1,2-dichloroethane, which is arbitrarily assigned an AN value of 100. Liquids with the higher acceptor numbers were considered to be more acidic.

Mayer and Gutmann chose hexane as a standard solvent, and any solvent in which the ^{31}P NMR shift for Et_3PO exceeded that observed in hexane was assigned an acceptor number. Thus, in principle, all saturated hydrocarbons above hexane would have AN values, and aromatic hydrocarbons were assigned larger AN values. Even appreciably basic liquids without electrophilic sites sufficient to promote self-association (and immiscibility in squalane), such as diethyl ether, tetrahydrofuran, dioxane, and pyridine, were assigned appreciable AN values. Such AN values have been difficult for experimentalists to accept, but the AN-AN^d values of Table III agree with laboratory experience.

It should be noted that the AN of 100 assigned to dilute solutions of antimony pentachloride in 1,2-dichloroethane is calculated from a δ_{corr} ^{31}P NMR shift for Et_3PO of 42.59 ppm referenced to Et_3PO solutions in *n*-hexane, so the total shift will include a van der Waals contribution of 5.69 ppm for hexane minus a 10.07 ppm van der Waals contribution for 1,2-dichloroethane, as shown in Table III. Thus, the acid-base contribution to this shift $\Delta\delta^{\text{ab}}$ is 38.21 ppm. Should we now use the shift of 38.21

ppm for the standard? If the values of acceptor numbers are to be changed to measure only acidity, perhaps it would be better to use units of kilocalories per mole, for as will be shown in paper 2 of this series, the acid-base contributions to the ^{31}P NMR shifts of Et_3PO are directly proportional to the heats of acid-base interaction of Et_3PO with acidic liquids, and then the new AN values (AN*) would be in the same units as DN values. With the use of -25.8 kcal/mol as the heat of acid-base interaction of Et_3PO with antimony pentachloride (the negative of the DN for Et_3PO) to correspond to the 38.21 ppm acid-base contribution to the NMR shift,

$$AN^* = 25.8(AN-AN^d)/(38.21 \times 2.348) = 0.288(AN-AN^d) \quad (13)$$

Values of AN* (in kilocalories per mole) are listed in Table III.

Conclusions

The experimental results in this study show that the van der Waals contribution to the ^{31}P NMR chemical shifts of Et_3PO are quite significant, as are also the infrared chemical shifts for the -P=O stretching peaks. When the ^{31}P NMR shifts are corrected by subtracting the van der Waals contribution, the resulting shifts ($\Delta\delta^{\text{ab}}$) and the corrected acceptor numbers AN-AN^d or of AN* (in kcal/mol) appear to be more reasonable, for only acids are found to have appreciable values of AN-AN^d or of AN*.

Acknowledgment. We acknowledge the support of this research by the Department of Energy (Grant No. DE-FG22-87PC9925) and by IBM (San Jose). Appreciation is expressed to Dr. T. B. Lloyd and to Prof. James E. Roberts for helpful discussions and contributions to this effort and to W. E. Pastore for the interfacial tension measurements.

Registry No. Et_3PO , 597-50-2.

Natural-Abundance Two-Dimensional Solid-State ^{29}Si NMR Investigations of Three-Dimensional Lattice Connectivities in Zeolite Structures

C. A. Fyfe,* Y. Feng, H. Gies, H. Grondey, and G. T. Kokotailo

Contribution from the Department of Chemistry, University of British Columbia, Vancouver, British Columbia, Canada. Received July 24, 1989

Abstract: The 3D lattice connectivities in zeolites ZSM-12 and KZ-2 have been investigated by natural-abundance $^{29}\text{Si}/^{29}\text{Si}$ COSY and INADEQUATE 2D NMR experiments. In both cases the results are in exact agreement with the lattice structures, the INADEQUATE experiment being particularly successful and detecting all of the connectivities. In addition, it is possible to observe directly the scalar *J* couplings that are in the range of 10–15 Hz. The approach is of quite general applicability and may be extended to other 3D structures.

Zeolites are porous aluminosilicates (tectosilicates) whose unique 3D tetrahedral framework structures incorporate cavities and interconnecting channel systems,¹ giving them a size and shape selectivity for sorbed organic molecules that makes them of considerable importance in industry as molecular sieves and as catalysts.² Although they are highly crystalline and their structures are often highly symmetrical, there are difficulties in determining their crystal structures by diffraction techniques. First, they are usually microcrystalline with particle dimensions of a only few micrometers, which precludes the simple application of single-crystal diffraction techniques, and recourse must be made to much more limited power diffraction data.³ Second, Si and

Al atoms have very similar scattering factors and, in addition, are often disordered within the framework of the zeolite so that even when the topology of the overall crystal structure can be

(1) (a) Breck, D. W. *Zeolite Molecular Sieves*; Wiley Interscience: New York, 1974. (b) Smith, J. V. *Zeolite Chemistry and Catalysis*; Rabo, J. A., Ed.; ACS Monograph 171; American Chemical Society: Washington, DC, 1976; p 3.

(2) (a) Barrer, R. M. *Zeolites and Clay Minerals as Sorbents and Molecular Sieves*; Academic Press: London, 1978. (b) Hölderich, W.; Hesse, M.; Näumann, F. *Angew. Chem.* **1988**, *27*, 226.

(3) (a) Information from powder diffraction data may be improved by use of Rietveld analysis and synchrotron X-ray sources. (b) The use of synchrotron X-ray sources makes it possible to work with much smaller crystals and may be generally applicable to zeolites in the future. Eisenberger, P.; Newman, J. B.; Leonowicz, M. E.; Vaughan, D. E. W. *Nature* **1984**, *309*, 45.

* To whom correspondence should be addressed.

found, it is generally not possible to locate the Si and Al atoms within the framework.

In recent years, $^{29}\text{Si}/^{27}\text{Al}$ MAS NMR spectroscopy has emerged as a complementary technique to X-ray diffraction measurements for the investigation of zeolite crystal structures.⁴ In the case of low Si/Al ratio materials, five resonances are observed (to a first approximation), corresponding to the five possible local environments Si[4Al], Si[3Al,Si], Si[2Al,2Si], Si[Al,3Si], and Si[4Si] describing the (average) local Si/Al distributions throughout the framework.⁵ In completely siliceous materials, where only the Si[4Si] local environment is present, very sharp resonances are observed that are due to the crystallographically inequivalent silicon sites in the unit cell and whose relative intensities reflect the relative site occupancies.⁶ These latter spectra may thus be directly related to the results of diffraction experiments and can be used to investigate unknown zeolite structures.

In solution NMR studies, the application of 2D techniques has provided a wealth of information on the 2D connectivities between atoms within molecular structures. For example, the HSC (heteronuclear shift correlation) sequence establishes heteronuclear connections such as $^{13}\text{C}/^1\text{H}$, $^{29}\text{Si}/^1\text{H}$, etc. Sequences such as COSY define homonuclear correlations such as $^1\text{H}/^1\text{H}$, $^{31}\text{P}/^{31}\text{P}$, $^{29}\text{Si}/^{29}\text{Si}$, etc., and the INADEQUATE sequence $^{13}\text{C}/^{13}\text{C}$ in natural abundance.⁷ Benn and co-workers have recently demonstrated $^{13}\text{C}-^{13}\text{C}$ connectivities using the INADEQUATE sequence for the plastic crystal camphor and have used the COSY sequence for $^{29}\text{Si}/^{29}\text{Si}$ connectivities in the reference molecule Q_8M_8 .⁸ At least in principle, 2D NMR techniques can be used to establish connectivities in the solid state, which for crystalline 3D framework structures (in contrast to the case of molecular crystals) could be used to define the 3D structure itself. In previous work we have demonstrated the viability of this approach for $^{29}\text{Si}-^{29}\text{Si}$ connectivities in zeolites, showing that both spin diffusion and COSY experiments yielded the expected 3D bonding scheme for the known lattice structure of zeolite ZSM-39.⁹ Of the two experiments, the latter is considered more reliable as the former is affected by non-distance-dependent factors, which in general will be difficult to estimate. In this previous study, a small sample of highly crystalline ZSM-39 was synthesized, which was enriched to approximately 80% in ^{29}Si to increase the S/N and enhance the connectivities due to the $^{29}\text{Si}-^{29}\text{Si}$ interactions. However, such high levels of enrichment will not, in general, be possible due to the expense involved, and the techniques must be refined so that they can be performed on natural-abundance samples if they are to be of general applicability. In the present paper we show how the information from the previous studies of enriched material may be used to develop an appropriate protocol for experiments on natural-abundance samples, and we present the results from a series of such experiments on two representative zeolite structures. A preliminary account of one of these experiments has been presented.¹⁰

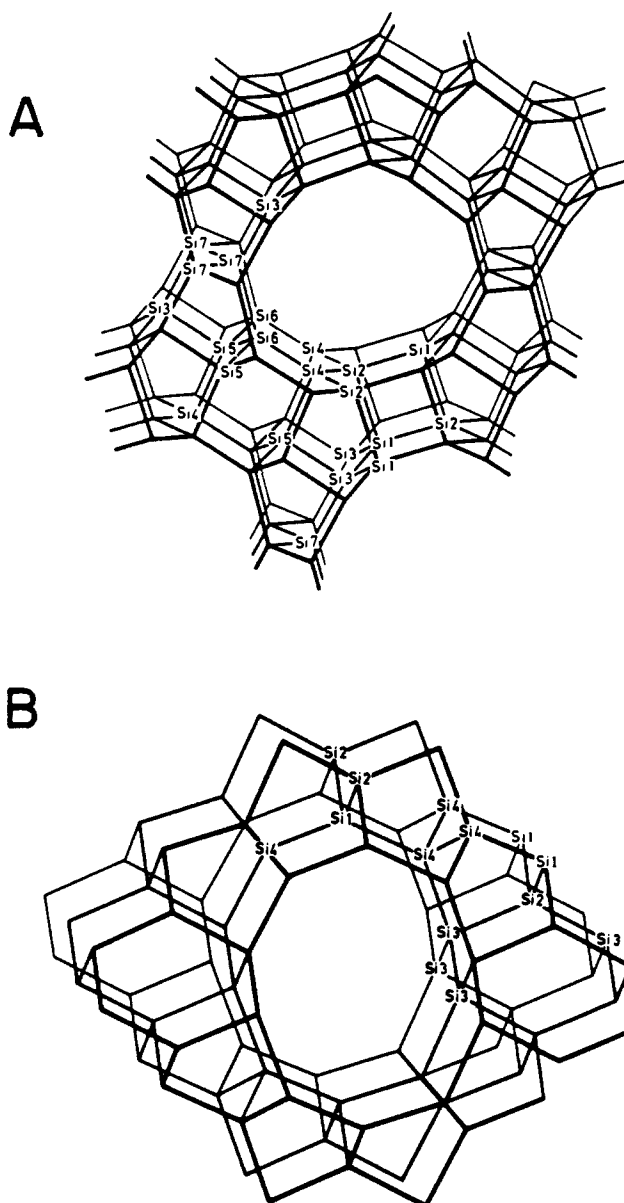


Figure 1. Schematic representation of the zeolite lattice framework: (A) ZSM-12, the seven crystallographically inequivalent tetrahedral lattice sites indicated by Si1, Si2, ..., Si7; (B) KZ-2, the four crystallographically inequivalent tetrahedral lattice sites indicated by Si1, Si2, Si3, and Si4.

Table I. T Sites, Their Occupancies, and Connectivities for the Asymmetric Unit in Zeolite ZSM-12

T site	occupancy	connectivity
T ₁	1	2T ₂ :2T ₃
T ₂	1	2T ₁ :2T ₄
T ₃	1	2T ₁ :1T ₅ :1T ₇
T ₄	1	2T ₂ :1T ₅ :1T ₆
T ₅	1	1T ₃ :1T ₄ :2T ₆
T ₆	1	1T ₄ :2T ₅ :1T ₇
T ₇	1	1T ₃ :1T ₆ :2T ₇

Experimental Section

^{29}Si MAS NMR spectra were obtained at 79.49 MHz with a Bruker MSL 400 spectrometer with the "magic angle" accurately set with the ^{79}Br resonance of KBr.¹¹ Standard pulse sequences were used for both relaxation time measurements and the various 2D experiments.⁷ Samples were spun at frequencies equal to, or a multiple of, the spectral sweep width so that any spinning sidebands that were not attenuated in F_1 were

(4) (a) A description of the range of applications of these experiments in chemical systems is given in: Fyfe, C. A. *Solid State NMR for Chemists*; CRC Press: Guelph, ON, 1984. (b) Engelhardt, G.; Michel, D. *High Resolution Solid-State NMR of Silicates and Zeolites*; John Wiley and Sons: New York, 1987.

(5) (a) Lippmaa, E.; Magi, M.; Samoson, A.; Tarmak, M.; Engelhardt, G. *J. Am. Chem. Soc.* **1981**, *103*, 4992. (b) Lippmaa, E.; Magi, M.; Samoson, A.; Engelhardt, G.; Grimmer, A. R. *J. Am. Chem. Soc.* **1980**, *102*, 4889. (c) Fyfe, C. A.; Thomas, J. M.; Klinowski, J.; Gobbi, G. C. *Angew. Chem.* **1983**, *95*, 257; *Angew. Chem., Int. Ed. Engl.* **1983**, *22*, 259.

(6) Fyfe, C. A.; Gobbi, G. C.; Murphy, W. J.; Ozubko, R. S.; Slack, D. A., *J. Am. Chem. Soc.* **1984**, *106*, 4435.

(7) (a) Benn, R.; Günther, H. *Modern Pulse Methods in High Resolution NMR Spectroscopy*. *Angew. Chem., Int. Ed. Engl.* **1983**, *22*, 250. (b) Bax, A. *Two Dimensional Nuclear Magnetic Resonance in Liquids*; Delft University Press: The Netherlands, 1982. (c) Derome, A. E. *Modern NMR Techniques for Chemistry Research*; Pergamon Press: New York, 1987. (d) Sanders, J.; Hunter, B. *Modern NMR Spectroscopy, A Guide for Chemists*; Oxford University Press: New York, 1987. (e) Kessler, H.; Gehrke, M.; Griesinger, C. *Angew. Chem., Int. Ed. Engl.* **1988**, *27*, 490.

(8) Benn, R.; Grondy, H.; Brevard, C.; Pagelot, A. *J. Chem. Soc., Chem. Commun.* **1988**, 102.

(9) Fyfe, C. A.; Gies, H.; Feng, Y. *J. Am. Chem. Soc.* **1989**, *111*, 7702.

(10) Fyfe, C. A.; Gies, H.; Feng, Y.; Kokotailo, G. T. *Nature* **1989**, *341*, 223.

(11) Frye, J. S.; Maciel, G. E. *J. Magn. Reson.* **1982**, *48*, 125.

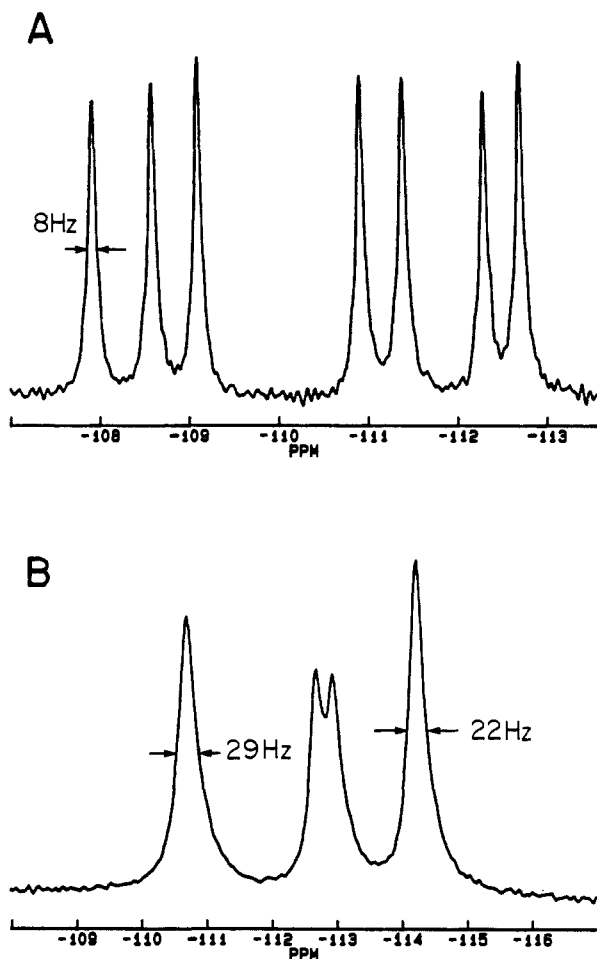


Figure 2. ^{29}Si MAS NMR spectra: (A) zeolite ZSM-12; (B) zeolite KZ-2 (ZSM-22).

exactly coincident with the main signals. Spinning rates were controlled to ± 5 Hz during the experiments with a standard Bruker spinning accessory.

Results and Discussion

A. General Procedure. The previous studies on ^{29}Si -enriched material suggested that the critical determining factor was the ^{29}Si T_2^* values as reflected in the spectral line widths, and samples with very narrow resonances were selected for study in the present work. The observed line widths at 79.46 MHz ranged between 10 and 30 Hz. The structures of the zeolites chosen for study, ZSM-12 and KZ-2, represent a range of complexity and are considered reasonably typical of this class of materials. Zeolite ZSM-12 is a 3D framework structure as illustrated in Figure 1A. The space group from the original structure determination¹² has been revised to $C2/c$ with a doubling of the C_0 unit cell parameter in a recent refinement of synchrotron powder X-ray data by Gies and co-workers,¹³ but the general features of the lattice are the same. The asymmetric unit consists of seven crystallographically inequivalent T sites as indicated in the figure with the connectivities between the different sites given in Table I. The ^{29}Si MAS NMR spectrum (Figure 2A) shows seven well-resolved peaks that are of exactly equal intensity when appropriately long recycle delays are used, in agreement with the site occupancies.

Zeolite KZ-2 has a 1D pore structure whose framework is shown in Figure 1B. There are four T sites in the asymmetric unit, of occupancies 2:1:1:2 as indicated in the figure.¹⁴ More

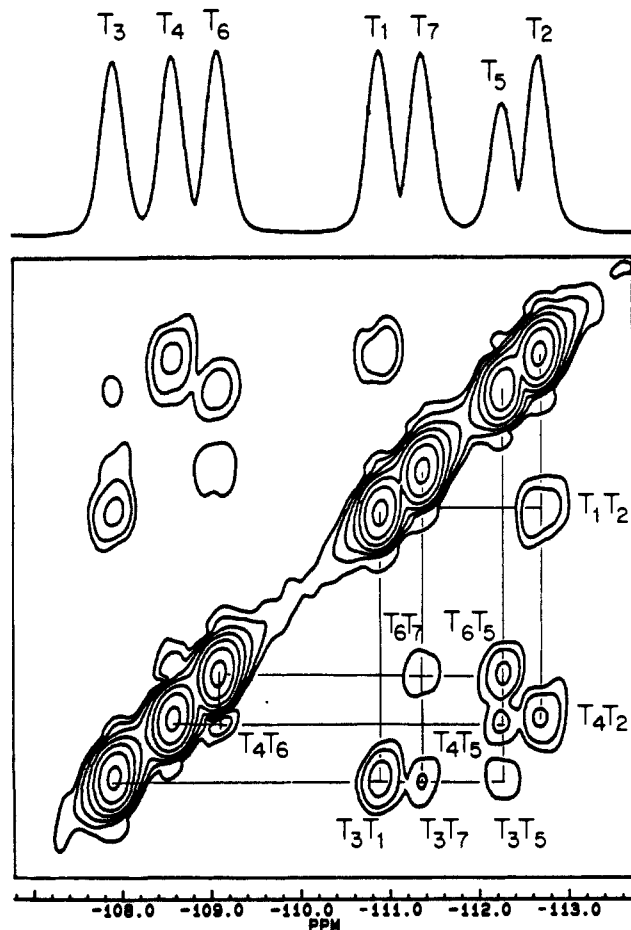


Figure 3. Contour plot of COSY experiment on zeolite ZSM-12 with a projection in the F_2 dimension carried out at 300 K with 64 experiments, 160 scans in each experiment, sweep width of 1200 Hz, and a fixed delay of 5 ms. 256 real data points, sine-bell-squared apodization, and magnitude calculation were used for data processing.

recently, refinements of the structure have been presented,¹⁵ and it has been demonstrated that the series of zeolites KZ-2, ZSM-22, θ -1, and NU-10 all have the same structure.¹⁶ The ^{29}Si NMR spectrum (Figure 2B) shows four resonances of relative intensities 2:1:1:2, in excellent agreement with the diffraction-determined structure.

B. COSY Experiments on ZSM-12 and KZ-2. COSY experiments were carried out with the conventional pulse sequence $[(90^\circ_x)-t_1-\tau-(90^\circ_x)-\tau-t_2, \text{acquire}]$,¹⁷ where t_1 is the phase-encoding step and τ is a fixed delay whose value is chosen to optimize the intensities of the connectivities. In the COSY-45 experiments, the second 90°_x pulse is reduced to between 45° and 60° . In all these experiments, the evolution time will be effectively limited by the T_2 or more properly the T_2^* of the ^{29}Si nuclei. From the observed line widths of ca. 9 Hz in the ^{29}Si MAS NMR spectrum of ZSM-12 (Figure 2A), the optimum encoding time for the simple COSY and COSY-45 experiments was estimated and confirmed as being approximately 60 ms. Figure 3 shows contour plots from a typical COSY-45 experiment on this sample with the number of data points in t_2 reduced to 256 before zero-filling. As can be seen from the plots, connectivities between the resonances are clearly observed in the unsymmetrized plot, S/N being traded off against resolution in the choice of the number of data points used in t_2 . The resonances may be assigned unambiguously from the expected connectivities given in Table I by trial and error, but a partial assignment from other data may also be used as a starting

(12) LaPierre, R. B.; et al. *Zeolites* **1985**, *5*, 346.

(13) Fyfe, C. A.; Gies, H.; Kokotailo, G. T.; Marler, B.; Cox, D. E. *J. Phys. Chem.*, in press, 1989.

(14) (a) Barri, S. A. J.; Smith, G. W.; White, D.; Young, D. *Nature* **1984**, *312*, 533. (b) Highcock, R. M.; Smith, G. W.; Wood, D. *Acta Crystallogr., Sect. C: Cryst. Struct. Commun.* **1985**, *C41*, 1391. (c) Kokotailo, G. T.; Schlenker, J. L.; Dwyer, F. G.; Valyocski, E. W. *Zeolites* **1985**, *5*, 349.

(15) Marler, B. *Zeolites* **1987**, *7*, 393.

(16) Fyfe, C. A.; Kokotailo, G. T.; Strobl, H.; Pasztor, C. S.; Barlow, G.; Bradley, S. *Zeolites* **1989**, *9*, 531.

(17) Muller, L.; Kumar, A.; Ernst, R. R. *J. Chem. Phys.* **1975**, *63*, 5490.

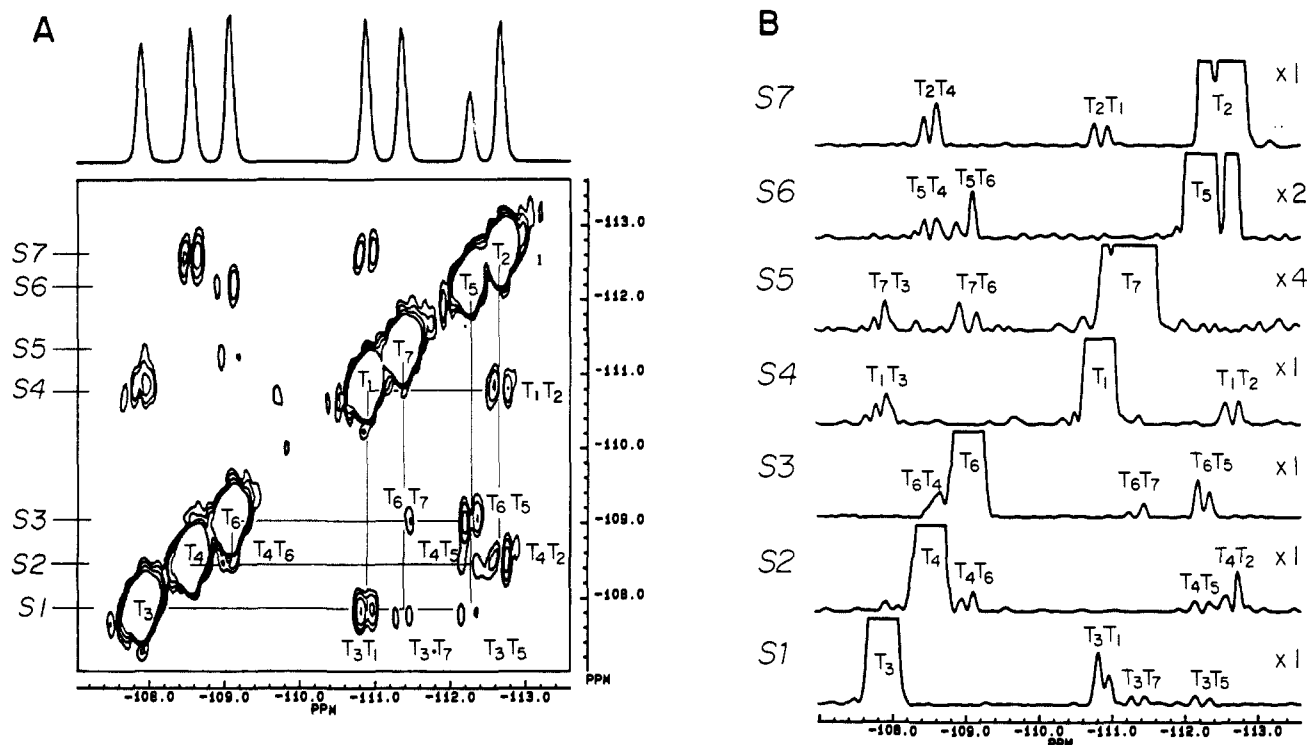


Figure 4. (A) Contour plot with projection in F_2 of a COSY experiment on ZSM-12 obtained under the same conditions as in Figure 3, except that there were 80 scans in each experiment and 450 data points and power calculation were used in the data processing. (B) Row plots from Figure 4A. The rows correspond to those indicated in Figure 4A.

Table II. T Sites, Their Occupancies, and Connectivities for the Asymmetric Unit in Zeolite KZ-2

T site	occupancy	connectivity
T_1	1	$2T_2:2T_4$
T_2	1	$2T_1:2T_3$
T_3	2	$1T_2:2T_3:1T_4$
T_4	2	$1T_1:1T_3:2T_4$

point for their assignment. Thus, some information may be gained from the expected correlation between the local geometries of the T sites, for example $\overline{T-T}$ distances and $T-O-T$ angles. However, considerable care must be taken with these data as there are very substantial errors in the powder diffraction derived structural parameters that vary over a limited range. Even in the best cases, these errors can easily be larger than the experimental differences in the parameters between sites with similar chemical shifts, and this could lead to quite wrong assignments. In the present instance, it is felt that the assignment of the signals within the two groupings in the spectrum is probably valid, but not the signals within the groups themselves. With use of data from the recent refinement by Gies and co-workers, the low-field grouping of lines is thought to comprise T_3 , T_4 , and T_6 while the high-field group of four lines is due to T_1 , T_2 , T_5 , and T_7 . Thus, an unambiguous assignment of one of the peaks may now be made when spectra are run without an adequate delay for complete recovery of the magnetization; the second highest field peak at -112.2 ppm is always of lower intensity, indicating that it has a longer T_1 value than the other resonances. This is confirmed by direct measurement of the T_1 values. Since a major contribution to the spin-lattice relaxation in these ^{29}Si systems is interactions of the silicon nuclei with molecular oxygen, this unambiguously identifies this resonance as being due to T_5 as this site (Figure 1A) is the only one that is not part of a channel surface and, therefore, will not be in contact with adsorbed oxygen. T_5 is connected to each of the resonances T_3 , T_4 , and T_6 , which from the 2D plots confirm the assignment of the grouping of low-field signals. T_7 is not connected to T_1 , T_5 , or T_2 , and thus from the plot T_7 may be assigned as the resonance at -111.4 ppm. T_7 is also connected to T_3 and T_6 , giving a partial assignment of these signals and assigning the resonance at -108.6 ppm as T_4 . T_2 has double connections to both T_1 and

T_4 , and since T_4 is known, the highest field resonance at -112.7 ppm must be T_2 . The higher intensities of the T_2T_1 and T_2T_4 cross-peaks are in agreement with the doubling of the connectivities. T_1 has double connections to T_2 and T_3 , and thus, T_3 (and hence T_6) may be assigned, the intensity of the T_1T_3 cross-peak again being in agreement with the double connectivity.

All of the resonances are now known, and the remaining cross-peaks may be assigned. All of the expected connectivities are quite clearly observed, ambiguity being T_4T_6 which lies close to the diagonal peaks. This can, however, be confirmed by other experiments.

When 450 points are used before zero-filling in t_2 there is some loss of S/N, but the cross-peaks clearly appear as doublets (Figure 4A). In principle, four peaks should be observed in each cross-peak, but the real digital resolution in F_1 without zero-filling is only ~ 20 Hz/point and is not sufficient to resolve splittings in this dimension. The structure of the cross-peaks may be clearly observed in plots of rows from the 2D spectrum as shown in Figure 4B. From the 4.6% natural abundance of ^{29}Si and its 4-fold coordination, the only spin-spin interactions in the first coordination sphere will be from $^{29}\text{Si}-\text{O}-^{29}\text{Si}$ pairs and these will comprise approximately 18% of the total ^{29}Si spectral intensity. The lattice thus consists of 95.4% non-NMR-active Si nuclei and 4.6% NMR-active nuclei. Of the latter, 82% exist as isolated uncoupled nuclei and 18% as isolated pairs of ^{29}Si nuclei that give rise to the connectivities. The magnitudes of the apparent couplings are in the range of 10–15 Hz, and they are symmetrical about the diagonal as expected. These values must be considered approximate due to the limited real digital resolution (~ 3 Hz/point) and the fact that the experiments are not phase-sensitive, which will tend to increase the observed splitting somewhat. However, the approximate values of about 10–15 Hz would seem to be a valid estimate, useful in planning further experiments. The mechanism for the interaction is thought to be scalar coupling, and the values observed are of the correct magnitude when compared with solution data from ^{29}Si -enriched silicate solutions.¹⁸ Values for $J_{\text{Si-Si}}$ from these studies range from 1 to 16 Hz, with

(18) Harris, R. K.; Knight, C. T. *J. Chem. Soc. Faraday Trans. 2* 1983, 1539, and references therein.

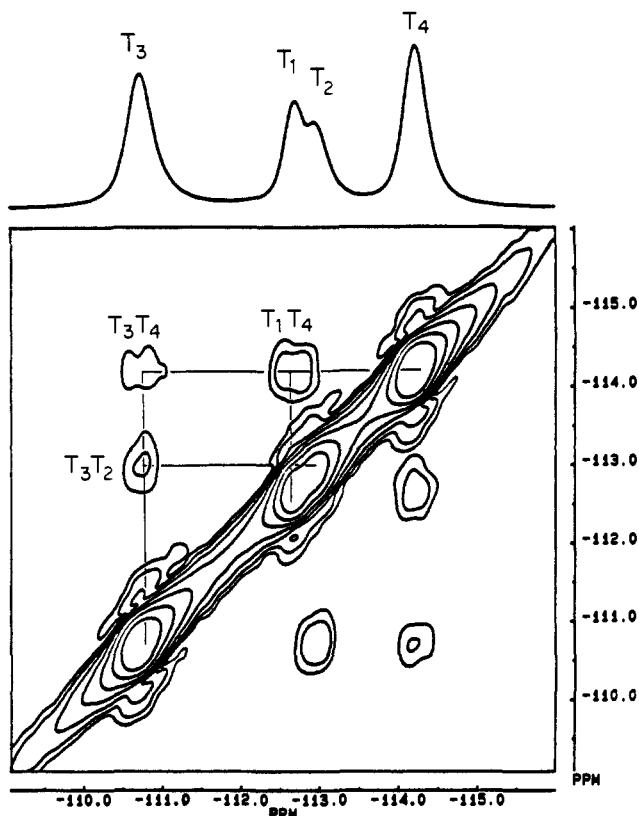


Figure 5. Contour plot with projection in the F_2 dimension of a COSY experiment on zeolite KZ-2 carried out at 300 K, 64 experiments, 592 scans per experiment, 1200 Hz sweep width, fixed delay of 0.5 ms. 256 data points were used during the data processing and sine-bell-squared apodization and magnitude calculation employed.

most being less than 10 Hz. However, most silicate species in solution contain a substantial number of three- and four-membered (T atom) rings, and the couplings are very dependent on ring size. When only data from four- and five-membered (T atom) rings are considered, the values range between 9 and 16 Hz, in excellent agreement with the present work. However, possible dipolar contributions must also be considered as there will be a homonuclear dipolar interaction within each $^{29}\text{Si}-\text{O}-^{29}\text{Si}$ pair that, for a powder sample, will give rise to two "Pake doublets" separated in chemical shift. Since the distance dependence of the dipolar interaction will effectively preclude the detection of $^{29}\text{Si}-\text{O}-\text{Si}-\text{O}-^{29}\text{Si}$ couplings (>5 Å) compared to $^{29}\text{Si}-\text{O}-^{29}\text{Si}$ interactions (~ 3 Å), and connectivity pattern similar to that from scalar couplings might be expected. The value of the Pake doublet splitting in the static powder can be calculated as 260 Hz from the magnetic moments and an assumed internuclear distance of 3 Å. The spinning rates at the magic angle used in the present studies ranged up to 3.6 kHz, but it is still possible that dipolar-derived spectral structure could be observed. Exact calculation of the effect involves a knowledge of the anisotropies (including their orientations, which are not available).^{19,20} However, the magnitude of the observed "coupling" depends inversely on the spinning rate. As a test of the possible contribution of dipolar interactions in the present work, experiments were carried out at 1.2 and 2.4 kHz. No differences in the magnitudes of the couplings were observed, and it is considered that this rules out the interactions being dipolar in nature. In addition, scalar couplings *must* be present, and the observed splittings are of the correct size from the values obtained in solution studies.

Similar results are obtained from experiments on zeolite KZ-2 whose 3D structure is shown in Figure 1B and are presented in Figures 5 and 6 in the same format as used above for ZSM-12.

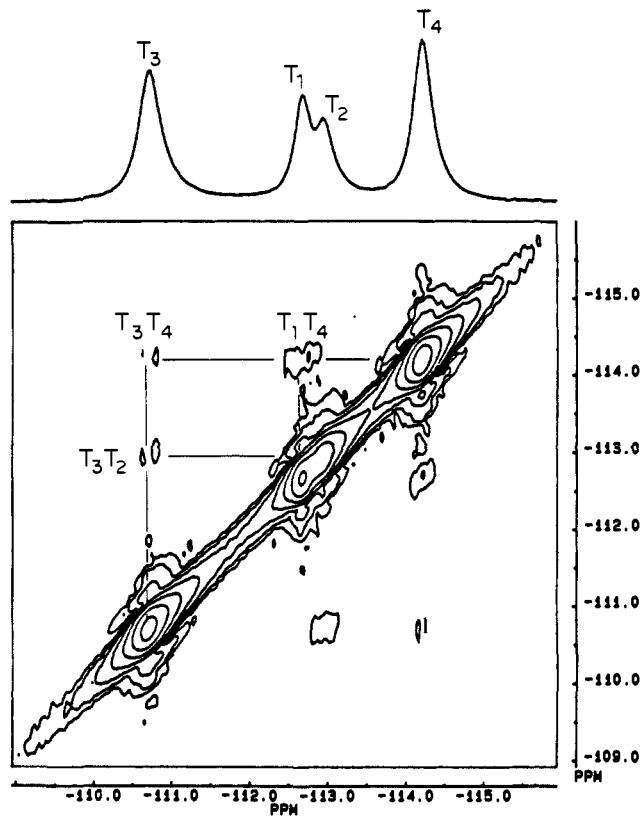


Figure 6. Contour plot with projection in F_2 of a COSY experiment on KZ-2. Conditions were the same as employed in Figure 5 except that 512 data points and sine bell apodization were used in the data processing.

The connectivities expected are presented in Table II. The resonances may be divided into two groups T_1, T_2 and T_3, T_4 on the basis of their relative intensities. (2 and 1, respectively). From the correlation between $\bar{T}-\bar{T}$ distance and chemical shift, from the X-ray structural data, the resonances of double intensity T_3, T_4 may be assigned such that T_3 is the lowest field signal at -110.6 ppm and T_4 is the highest field signal at -114.2 ppm. The large difference in chemical shift between these two signals makes the assignment reliable, but the method cannot be used to distinguish the two inner signals. From the assignments of T_3 and T_4 and the expected T_3T_2 and T_4T_1 connectivities, the resonances T_1 and T_2 may be assigned as indicated. In addition to the expected T_3T_4 connectivity that is observed, a connectivity between T_1 and T_2 is expected, but the cross-peaks are too close to the diagonal to be resolved. They are, however, detected in other experiments (see later text). When 512 points are used in F_2 before zero-filling, doublet structure is observed in the cross-peaks as in the case of ZSM-12, but the S/N is not as good. The values of the splittings are again in the range 10–15 Hz, and they are symmetrical about the diagonal as expected. As in the case of ZSM-12 discussed above, the mechanism is thought to be scalar J coupling.

C. INADEQUATE Experiments. The 2D INADEQUATE experiments in the present work were carried out with a conventional $[(90^\circ_x)-\tau-(180^\circ)-\tau-(90^\circ_x)-t_1-(135^\circ)-t_2, \text{acquire}]$ sequence²¹ where the value of τ is chosen to maximize the connectivities for a particular J coupling value. Compared to the COSY experiment, the INADEQUATE experiment has a number of advantages and disadvantages: In general, better S/N may be anticipated as there is a 2-fold decrease in the multiplicities of the cross-peaks, the main (noncoupled) center signals are subtracted, giving better dynamic range for the connectivities, and since the final signal is more constant in time, a much more efficient filter function can be used. In addition, any spinning

(19) Maricq, M. M.; Waugh, J. S. *J. Chem. Phys.* **1979**, *70*, 3300.

(20) Kubo, A.; McDowell, C. A. *J. Chem. Soc., Faraday Trans. 1* **1988**, *84*, 3713.

(21) (a) Bax, A.; Freeman, R.; Frenkiel, T. A.; Levitt, M. H. *J. Magn. Reson.* **1981**, *43*, 478. (b) Marci, T. H.; Freeman, R. *J. Magn. Reson.* **1982**, *48*, 158.

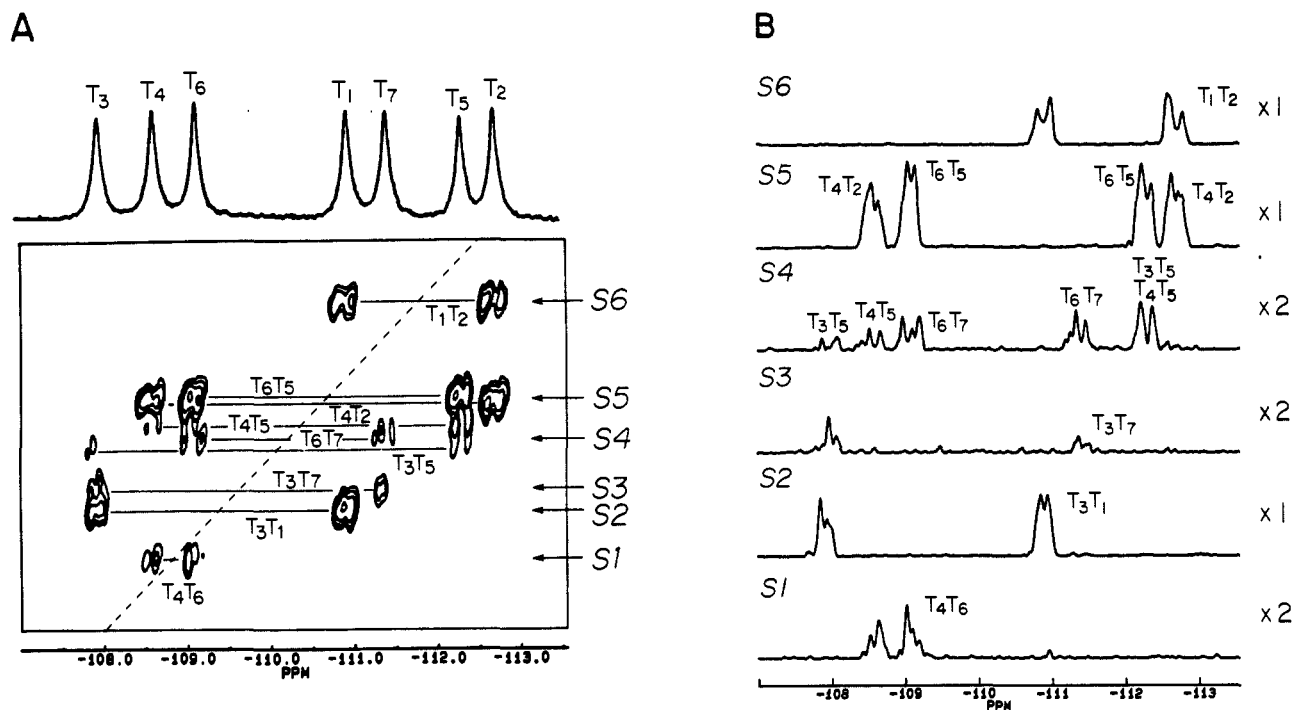


Figure 7. (A) Contour plot of INADEQUATE experiment on ZSM-12 at 300 K with the 1D MAS NMR spectrum shown above with 52 experiments carried out, 64 scans per experiment, 800 Hz sweep width, fixed delay of 20 ms, and 450 data points collected during the acquisition. Sine bell apodization and power calculation were used in the data processing. (B) Row plots from Figure 7A. The numbers of the rows correspond to those indicated in Figure 7A.

rate may be used, as spinning sidebands will not appear in the 2 dimensions after analysis of the data and it is much easier to observe connectivities between resonances close in frequency which occur close to the large diagonal signals in the COSY experiment. The main potential disadvantage of the technique is that one must have a reasonable estimate of the scalar J coupling to choose the appropriate value of τ . If this can be done, all of the individual frequency-encoding experiments make an efficient contribution to the experiment, resulting in good S/N as noted above. If the J coupling is not known, all of the individual experiments will be inefficient whereas a corresponding COSY experiment or selected portions of it will yield some information. In addition, the situation may arise where the values of the relaxation times and couplings are such that it is not possible to have a long enough evolution time. However, in the present work, the J coupling values are known from the previous experiments, and the line widths of the resonances (and the associated T_2^* and longer T_2 values) are such that they impose no severe restraints on the experiments, so that well-defined correlations are obtained with quite acceptable S/N.

Figure 7A shows the results of an INADEQUATE experiment²¹ on ZSM-12 carried out with the experimental parameters given in the figure caption with the delay τ chosen assuming the J couplings were between 10 and 15 Hz. All of the connectivities found and assigned in the previous COSY experiments are confirmed, including that between T_4 and T_6 , which is clearly resolved here but was ambiguous in the COSY experiment due to the close proximity of the cross-peaks to the diagonal. It should be noted that all of the assignments previously discussed could just as easily have been made from the INADEQUATE experiment, the observation of the T_4T_6 connection giving increased confidence in the assignment as every single connectivity is now observed. As previously, the intensities of the signals qualitatively reflect the numbers of connections involved. The doublet structures are clearly observable in this experiment, again confirming the previous results. The resolved splittings from single rows in the 2D plot (Figure 7B) are in good agreement with the values previously found and do not change when the spinning rate is varied between 1.0 and 3.0 kHz. Similar results are found for zeolite KZ-2 as shown in Figure 8. Again the connectivities previously observed are confirmed, and the T_1T_2 coupling not observed at all in the COSY experiments (Figures 5 and 6) is now clearly seen. All

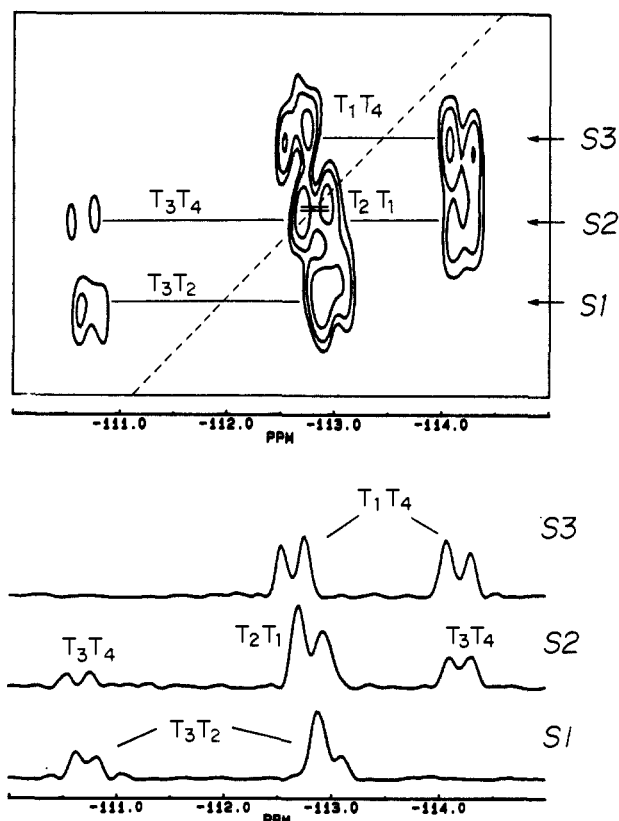


Figure 8. Contour plot of INADEQUATE experiment on zeolite KZ-2 with three individual rows shown as indicated. The experiments were carried at 300 K, 16 experiments, 256 scans for each experiment, 750 Hz sweep width, fixed delay of 20 ms, and 200 data points collected. Sine bell and trapezoidal apodization were used for the F_2 and F_1 dimensions, respectively, in the data processing.

of the signals exhibit a doublet structure, and the interactions have values similar to those previously observed in the COSY experiments. Again, a complete assignment of all of the connectivities in the structure is obtained, and this would have been possible

even if the results of the COSY experiments were not known.

D. Conclusions. The present work has thus demonstrated for two representative zeolite structures that it is possible to perform reliable 2D COSY and INADEQUATE experiments in natural abundance. Although the T_2 values are of the order of seconds in these systems, and are much larger than the T_2^* values, the line widths are such that they impose no real constraints on the experiments. All of the anticipated $^{29}\text{Si}-^{29}\text{Si}$ interactions are observed, detailing the complete 3D connectivities in the two structures. In addition, the couplings, thought to be scalar in nature, between the $^{29}\text{Si}/^{29}\text{Si}$ spin pairs are observed and have "apparent" values of 10-15 Hz. The techniques may be considered of quite general applicability and will be useful in the investigation of other 3D-bonded solid-state structures. In this regard, it is useful to consider the information now available from the NMR studies alone. For example in the case of ZSM-12 we would know that the unit cell contained seven inequivalent T sites of equal occupancies, one of which was "buried" in the walls of the structure, and all of the connectivities given in Table I. Bearing in mind that the total of the connectivities to a given T site must be four, and that the cross-peak intensities qualitatively reflect the numbers of connections, some estimates could also be made

on the numbers of the different connectivities present. Taken together with other experimental data, for example for sorption studies, these results would be very useful in discriminating between different proposed structures and, in favorable cases, might even be used to generate possible structures for comparison with experimental powder X-ray diffraction data.

The results also make it possible to predict from magnitudes of the observed scalar couplings that the simple experiments described will not be unduly constrained by T_2^* values for systems with line widths of approximately 30 Hz or less and that useful data may be obtained from COSY experiments for even broader resonances. It should be possible, for extreme cases where $T_2 \gg T_2^*$ in the solid state, to generate more efficient versions of the COSY experiment. Work in this area is currently in progress as are studies of a number of other zeolite systems.

Acknowledgment. We acknowledge the financial assistance of the NSERC (Canada) in the form of operating and equipment grants (C.A.F.) and the Alexander von Humboldt Foundation (H.G., G.T.K.). C.A.F. acknowledges the award of a Killam Research Fellowship by the Canada Council and Y.F. the award of a University Graduate Scholarship.

Thermal- and Light-Induced Spin Transition in $[\text{Fe}(\text{mtz})_6](\text{BF}_4)_2$: First Successful Formation of a Metastable Low-Spin State by Irradiation with Light at Low Temperatures[†]

P. Poganiuch,[‡] S. Decurtins,[§] and P. Gülich*

Contribution from the Institut für Anorganische Chemie und Analytische Chemie, Johannes Gutenberg-Universität Mainz, Staudinger Weg 9, D-6500 Mainz, FRG. Received July 31, 1989

Abstract: The iron(II) spin-crossover complex $[\text{Fe}(\text{mtz})_6](\text{BF}_4)_2$ (mtz = 1-methyl-1H-tetrazole) has two different iron(II) lattice sites A and B. The ^{57}Fe Mössbauer spectra of the compound consist of only one quadrupole doublet above ~ 160 K, which is typical for iron(II) in the high-spin (HS) state. This indicates that the two sites A and B are indistinguishable above this temperature. Below ~ 160 K two different doublets are observed, both arising from iron(II) in the HS state. Several reasons for this phenomenon are discussed. Only the complex molecules, or rather the metal ions, in lattice site A undergo thermal spin transition to the low-spin (LS) state of iron(II), whereas those in lattice site B remain in the HS state down to 4.2 K. By irradiation with light of a Xe arc lamp ($\lambda \sim 350$ -650 nm) at 20 K the well-known LIESST (light-induced excited spin state trapping) effect is observed for the lattice site A ions. A metastable HS state is formed, which has a practically infinitely long lifetime below 40 K. Irradiation of $[\text{Fe}(\text{mtz})_6](\text{BF}_4)_2$ with red light ($\lambda > 700$ nm) at 20 K causes a light-induced HS \rightarrow LS conversion at lattice site B. The populated LS state is also metastable with a practically infinitely long lifetime below 50 K. This is the first example for a successful light-induced formation of a metastable LS state in an iron(II) HS complex.

1. Introduction

Temperature-dependent spin transition (spin crossover) is a well-established phenomenon in the coordination chemistry of first-row transition elements. Many examples are known, particularly for iron(II) compounds for which thermal low-spin (LS) \rightleftharpoons high-spin (HS) transition has been extensively studied, employing various techniques.^{1,2}

A few years ago, Decurtins et al.^{3,4} showed that in iron(II) spin-crossover complexes light-induced LS (1A_1) \rightarrow HS (3T_2) conversion can be observed by irradiation with green light ($\lambda \sim 550$ nm) into the $^1A_1 \rightarrow ^1T_1$ ligand field absorption band at

temperatures well below the thermal transition temperature. A mechanism for this phenomenon, denoted as "light-induced excited spin state trapping" (LIESST), was proposed.⁴ Figure 1 shows the potential energy surfaces of the low-lying ligand field states for a d^6 system with ligand field strengths in the region of spin crossover.⁵ The mechanism involves intersystem crossing from the excited 1T_1 state to an intermediate low-lying 3T_1 state and from there to the 3T_2 state, where at sufficiently low temperatures

(1) Goodwin, H. A. *Coord. Chem. Rev.* 1976, 18, 293.

(2) Gülich, P. *Struct. Bonding (Berlin)* 1981, 44, 83.

(3) Decurtins, S.; Gülich, P.; Köhler, C. P.; Spiering, H.; Hauser, A. *Chem. Phys. Lett.* 1984, 105, 1.

(4) Decurtins, S.; Gülich, P.; Hasselbach, K. M.; Hauser, A.; Spiering, H. *Inorg. Chem.* 1985, 24, 2174.

(5) Sugano, S.; Tanabe, Y.; Kamiura, K. *Multiplets of Transition Metal Ions*; Academic Press: New York, 1970; p 110 ff. Tanabe, Y.; Sugano, S. *J. Phys. Soc. Jpn.* 1954, 9, 753.

* To whom correspondence should be addressed.

[†] Dedicated to Professor D. Reinen on occasion of his 60th birthday.

[‡] Present address: Department of Chemistry, Massachusetts Institute of Technology, Cambridge, MA 02139.

[§] Present address: EMS-Chemie, CH-7013 Domat/Ems, Switzerland.